Adapting Lateral Stepping Control to Walk on Winding Paths

Anna C. Render [a], Joseph P. Cusumano [b], Jonathan B. Dingwell [a,*]

[a] Department of Kinesiology, The Pennsylvania State University, University Park, PA 16802 USA
[b] Department of Engineering Science & Mechanics, The Pennsylvania State University, University Park, PA 16802 USA

* Corresponding Author: Jonathan B. Dingwell; Email: dingwell@psu.edu

---

CRediT Author Statement

Anna C. Render: Conceptualization, Data Curation, Formal Analysis, Investigation, Methodology, Software, Validation, Visualization, Writing – Original Draft, Writing – Review & Editing.

Joseph P. Cusumano: Conceptualization, Formal Analysis, Funding Acquisition, Methodology, Supervision, Writing – Review & Editing.

Jonathan B. Dingwell: Conceptualization, Data Curation, Formal Analysis, Funding Acquisition, Methodology, Project Administration, Resources, Supervision, Validation, Writing – Review & Editing.

CONFLICT OF INTEREST

The authors declare that there is no conflict of interest associated with this work.

ACKNOWLEDGEMENTS

The authors thank Dr. David M. Desmet and Dr. Meghan E. Kazanski for their contributions and technical support throughout data collections. This work was supported by NIH grants 1-R01-AG049735 & 1-R21-AG053470 to JBD & JPC.

ABSTRACT

Most often, gait biomechanics is studied during straight-ahead walking. However, real-life walking imposes many turns and/or other maneuvers people must navigate. Such maneuvers challenge people's lateral balance and can frequently induce falls. Determining how people regulate their stepping movements to maintain balance during complex walking tasks is therefore essential. Here, 24 adults (12F/12M; Age 25.8±3.5yrs) walked on wide or narrow virtual paths that were either straight, slowly-winding, or quickly-winding. From each trial, we computed time series of step widths and lateral positions relative to the path. We applied our Goal Equivalent Manifold framework to quantify how participants adjusted their lateral stepping and step-to-step corrections of step width and lateral position as they walked on these different paths. On the narrower paths, participants walked with narrower steps and less lateral position variability. They did so by correcting step-to-step deviations in lateral position more, while correcting step-to-step deviations in step width less. On the winding paths, participants took both narrower and more variable steps. Interestingly, on slowly-winding paths, participants corrected step-to-step deviations in step width more by correcting step-to-step deviations in lateral position less: i.e., they prioritized maintaining step width over position, likely to maintain lateral balance. Conversely, on quickly-winding paths, participants strongly corrected step-to-step deviations in both step width *and* lateral position: i.e., they prioritized maintaining both approximately equally, consistent with trying to maximize their maneuverability. These findings have important implications for persons with gait impairments who may have elevated fall risk.

INTRODUCTION

Most of what we know about gait biomechanics comes from studying how people walk in straight lines (Richards et al., 2023). However, real-life walking environments are far more complex, with natural and built features like uneven terrain (Matthis et al., 2018), and various fixed (Twardzik et al., 2019) or moving (Moussaïd et al., 2011) obstacles. This means people rarely walk straight-ahead for extended periods in real life (Orendurff et al., 2008). Instead, most all of our walking tasks involve frequent turns and/or other maneuvers (Glaister et al., 2007; Ho et al., 2023). Our ability to perform such non-straight walking tasks and seamlessly adjust our walking to diverse conditions illustrates the inherent adaptability of human locomotion.

Adaptability is crucial to human locomotion (Desmet et al., 2022). First and foremost, people must be able to take steps. This involves processes that govern within-step dynamics to ensure viability (i.e., to prevent falling) (Patil et al., 2022). While viability is necessary to walk, it is not sufficient. People walk with a destination to reach and/or other tasks to achieve (Arechavaleta et al., 2008): i.e., they walk with some purpose. Thus, people must also coordinate their steps to achieve *goal-directed* walking. Among the simplest of goals is to merely follow some designated path (Dingwell et al., 2023; Pham et al., 2011), like a sidewalk or store aisle, etc. Additionally, people also need to be able to respond to changes in walking conditions or task demands (Olivier et al., 2013).

Within the goal-directed or "regulation" level of locomotion, people adjust mediolateral foot placement from step to step to prevent lateral instabilities (Bruijn and van Dieën, 2018; Kuo, 1999; MacKinnon and Winter, 1993; Townsend, 1985). Since people naturally exhibit greater instability in the frontal plane (Bauby and Kuo, 2000; McAndrew et al., 2011), it is imperative to characterize how people coordinate these lateral foot placements. We developed a framework, based on Goal Equivalent Manifolds (GEMs) (Cusumano and Cesari, 2006; Cusumano and Dingwell, 2013), to propose and test specific hypotheses about how people regulate successive stepping movements to achieve straight-ahead walking (Dingwell and Cusumano, 2019; Dingwell et al., 2010). To regulate lateral stepping during walking, our GEM approach identified a need for people to multi-objectively regulate the combination of lateral body position (z_B) to remain on their specified path (Dingwell et al., 2023), and step width

(w) to maintain lateral balance (Dingwell and Cusumano, 2019). We also identified a tradeoff between z_B-regulation and w-regulation: one cannot easily prioritize one without de-prioritizing the other (Dingwell and Cusumano, 2019). During straight-ahead walking, people strongly prioritize w-regulation (Dingwell and Cusumano, 2019; Kazanski et al., 2020, 2023).

However, to walk without falling across different contexts, people must adapt their lateral stepping regulation. Striking the right balance between regulating z_B and w depends on the specific walking conditions/task. When people were given explicit task feedback to regulate either z_B or w from step to step, they traded off their prioritization by increasing error correction of the feedback task variable, while decreasing error correction of its complement (Render et al., 2021). People similarly traded off these priorities to perform discrete lateral lane changes (Desmet et al., 2022; Desmet et al., 2024), and while walking on continuously narrowing paths (Kazanski et al., 2023). However, when subjected to random external lateral perturbations, people increased error correction of both z_B and w (Dingwell et al., 2021; Kazanski et al., 2020). Importantly, none of these prior experiments assessed how people adapt lateral stepping while performing tasks that implicitly demand continuous modulation of both z_B and w regulation.

Here, we tasked young healthy adults to navigate various wide or narrow winding paths. Presenting people with paths of different widths challenged their ability to regulate their step widths (w). Making these paths oscillate laterally further challenged their ability to regulate their lateral position (z_B). Thus, we created walking paths that systematically challenged people to weigh how they prioritize both w and z_B simultaneously. By amplifying the inherent competition between maintaining w and z_B, we expected participants to implicitly adapt their lateral stepping regulation to accommodate both factors while navigating these paths. We predicted that on narrower paths, people would trade off decreased w-regulation for increased z_B-regulation, similar to what people do on continuously narrowing paths (Kazanski et al., 2023). However, as these paths get sufficiently difficult (narrow and oscillating more quickly), we predicted people would simultaneously increase their degree of error correction of both z_B and w, similar to when they are laterally perturbed (Kazanski et al., 2020).

METHODS

Participants

Prior to participation, all participants provided written informed consent, as approved by the Institutional Review Board of The Pennsylvania State University. Twenty-four young healthy people (Table 1) participated. Participants were screened to ensure no medications, lower limb injuries, surgeries, musculoskeletal, cardiovascular, neurological, or visual conditions affected their gait.

[Insert Table 1 About Here]

Assessments

We evaluated participants' balance using the Four Square Step Test (FSST; Table 1) (Dite and Temple, 2002). Each participant completed three trials and we recorded their mean time. We assessed participants' attention and processing speed using the Four-Choice Response Task (4CRT; Table 1), administered using PEBL software (https://pebl.sourceforge.net/) (Mueller and Piper, 2014). Each participant completed two blocks of 50 stimuli and we recorded their mean reaction time.

Experimental Protocol

Participants walked in a M-Gait virtual reality system (Motek Medical, Netherlands; Fig.1A) equipped with a 1.2 m wide treadmill. Each participant wore a safety harness secured to the ceiling overhead. For all walking trials, treadmill speed was set to 1.2 m/s with matched optic flow speed. Participants initially walked 4-minutes to

acclimate to the system.

We tasked participants to walk on paths projected onto the treadmill belt (Fig. 1B). We systematically manipulated both path oscillation frequency and width. We created pseudo-randomly oscillating paths using a sum of three sin waves with incommensurate frequencies:

$$z(x) = 0.22\sin(A \cdot 0.46875x) + 0.05\sin(A \cdot 0.625x) + 0.03\sin(A \cdot 0.9375x), \quad (1)$$

where z is the lateral position (in meters) of the path center, A is a frequency scaling factor, and x is forward treadmill distance (in meters). We presented participants with each of three oscillation frequency combinations: straight (STR: $A = 0$), low frequency (LOF: $A = 1$), and high frequency (HIF: $A = 4$). Each such path was presented at each of two widths, wide (W = 0.60 m) and narrow (N = 0.30 m), resulting in six unique paths (Fig. 1C). For each, we instructed participants to "stay on the path" and encouraged them to minimize stepping errors. They received visual (firework) and auditory (flute) penalties when steps landed outside the path boundaries. For each condition, participants completed a 1-minute introductory trial, followed by two 4-minute experimental trials. Order of presentation between conditions was counterbalanced across participants using a Latin Square design to reduce order effects. To minimize fatigue, participants were allowed to rest as needed after each trial.

[Insert Figure 1 About Here]

Data Processing

Each participant wore 16 retroreflective markers: four around the head, four around the pelvis (left/ right PSIS and ASIS), and four on each of the left and right shoes (aligned with first and fifth metatarsal heads, lateral malleolus, and calcaneus). Kinematic data were collected at 100 Hz from a 10-camera Vicon motion capture system (Oxford Metrics, Oxford, UK) and post-processed using Vicon Nexus software. Marker trajectories and path data from D-Flow software (Motek Medical, Netherlands) were analyzed in MATLAB (MathWorks, Natick, MA).

We only analyzed the two 4-minute experimental trials for each condition. Marker trajectory data were first low-pass filtered (4th-order Butterworth, cutoff: 10 Hz), then interpolated to 600 Hz to ensure accurate stepping-event detection (Bohnsack-McLagan et al., 2016). Heel strikes were determined using a marker-based algorithm (Zeni et al., 2008).

For each trial, we used the lateral locations of the left and right heel markers to define time series of left and right lateral foot placements. We calculated relevant lateral stepping variables in path-based coordinates (Dingwell et al., 2023). At each step, we aligned the path-based local coordinate system, $[x', z']$, to be tangent to the point on the path closest to the midpoint between the two heel markers for that step. Then, we then computed lateral body position as $z_{Bn} = ½(z'_{Ln} + z'_{Rn})$, and step width as $w_n = z'_{Rn} - z'_{Ln}$ (Fig 2A). This yielded time series of path-aligned $\{z_{Bn}, w_n\}$ for all steps $n \in \{1, \ldots, N\}$ (Fig. 2B) throughout a trial. For consistency, we analyzed the last $N = 300$ steps of each trial.

[Insert Figure 2 About Here]

Stepping Parameters

For each trial performed by each participant under each condition, we first computed within-trial means (μ) and standard deviations (σ) from the 300-step time series of both lateral body position (z_B) and step width (w).

We applied a two-factor (Frequency × Width) mixed-effects analyses of variance (ANOVA) with repeated measures to test for differences between conditions for each variable: $\mu(z_B)$, $\mu(w)$, $\sigma(z_B)$ and $\sigma(w)$. When main effects or interaction effects were found to be significant, we performed Tukey's pairwise post-hoc comparisons to test for differences between path frequencies (STR, LOF, HIF) for each path width (W, N) and between path widths for each path frequency. We conducted all statistical analyses in Minitab (Minitab, Inc., State College, PA).

Linear Error Correction

We performed linear error correction analyses (Dingwell and Cusumano, 2015) to quantify the extent to which participants corrected step-to-step deviations in z_B and w on subsequent steps. We presume people try to maintain some constant mean q^* for each $q \in \{z_B, w\}$. On any given step, n, they will exhibit some small deviation, $\tilde{q}_{(n)} = \left(q_{(n)} - q^*\right)$, from their desired mean. They would then be expected to correct those deviations on the subsequent step: $\Delta q_{(n+1)} = q_{(n+1)} - q_{(n)}$. We directly quantified the extent to which $\tilde{q}_{(n)}$ deviations were corrected by $\Delta q_{(n+1)}$ (Dingwell and Cusumano, 2015). For each $q \in \{z_B, w\}$ time series, we plotted the corrections ($\Delta q_{(n+1)}$) against their corresponding deviations $\left(\tilde{q}_{(n)}\right)$ and computed linear error correction slopes, $M(q)$, from these plots (Fig. 2C). Slopes equal to −1 indicate deviations that are completely corrected at the next step. Conversely, slopes approaching 0 indicate deviations that go uncorrected.

We applied the same two-factor (Frequency × Width) mixed-effects analyses of variance (ANOVA) as described above for each variable: $M(z_B)$ and $M(w)$. When main effects or interaction effects were found to be significant, we again performed relevant Tukey's pairwise post-hoc comparisons as described above.

GEM-Relevant Variance

Any step-to-step regulation of z_B and/or w must be enacted by taking steps: z_L and z_R. By their definitions (Dingwell and Cusumano, 2019), $\{z_B, w\}$ are related to $\{z_L, z_R\}$ as:

$$\begin{bmatrix} z_L \\ z_R \end{bmatrix} = \begin{bmatrix} 1 & -\frac{1}{2} \\ 1 & -\frac{1}{2} \end{bmatrix} \begin{bmatrix} z_B \\ w \end{bmatrix}. \tag{2}$$

We can thus visualize the effects of the above stepping regulation processes by plotting steps in the $[z_L, z_R]$ plane (Dingwell and Cusumano, 2019). This $[z_L, z_R]$ plane exhibits two, mutually perpendicular Goal Equivalent Manifolds (GEMs) (Cusumano and Cesari, 2006; Cusumano and Dingwell, 2013). One corresponds to maintaining constant position (z_B^*) (Fig. 2D; green), the other to constant step width (w^*) (Fig. 2D; blue). We expect how people prioritize their stepping regulation (i.e., error correction) should thus structure the variance in the $[z_L, z_R]$ plane accordingly. During straight walking, people strongly correct errors in w but not in z_B, thus exploiting the equifinality available along the w^* GEM to exhibit much larger variances in z_B than in w (Dingwell and Cusumano, 2019). Conversely, people executing lateral lane change maneuvers exhibit more isotropic variance distributions at their transition step (Desmet et al., 2024). Here, we therefore calculated the ratio $\sigma(z_B)/\sigma(w)$, where strong prioritization of w-regulation over z_B-regulation is expected to yield $\sigma(z_B)/\sigma(w) \gg 1$.

We applied the same two-factor (Frequency × Width) mixed-effects analyses of variance (ANOVA) as described above for $\sigma(z_B)/\sigma(w)$. As warranted, we again performed relevant Tukey's pairwise post-hoc comparisons as described above.

Correlations With Baseline Measures

To determine the extent to which baseline tests (FSST and/or 4CRT; Table 1) could predict walking task performance, we correlated these measures against our primary walking outcomes ($M(z_B)$, $M(w)$, and $\sigma(z_B)/\sigma(w)$)

for the Narrow HIF path condition, as this was the most balance-challenging condition presented.

RESULTS

Stepping Parameters

Participants exhibited similar mean values of z_B across all conditions ($p > 0.08$; Fig. 3A; Table 2), thus staying close to the center of each path. On the narrow paths, participants took narrower steps on average, $\mu(w)$, for all path frequency conditions ($p < 0.001$; Fig. 3B; Table 2). As path oscillation frequency increased (from STR to LOF to HIF) for both path widths, participants exhibited progressively narrower $\mu(w)$ ($p \leq 0.001$; Fig. 3B; Table 2).

[Insert Figure 3 About Here]

On the narrow paths, participants exhibited significantly less lateral position variability, $\sigma(z_B)$, for all path frequencies ($p < 0.001$; Fig. 4A; Table 2) and significantly less step width variability, $\sigma(w)$, on both the LOF and HIF paths ($p \leq 0.011$; Fig. 4B; Table 2). As path oscillation frequency increased for both path widths, participants exhibited significantly increasing $\sigma(z_B)$ ($p < 0.001$; Fig. 4A; Table 2) and $\sigma(w)$ ($p \leq 0.011$; Fig. 4B; Table 2).

[Insert Figure 4 About Here]

Linear Error Correction

Across all path frequency and path width combinations, participants consistently exhibited stronger error correction (slopes, M, closer to -1.0) for step width (w) deviations (Fig. 5C-D) than for lateral position (z_B) deviations (Fig. 5A-B), consistent with prior findings (Dingwell and Cusumano, 2019; Kazanski et al., 2023). On the narrow paths, participants corrected position deviations more, $M(z_B) \rightarrow -1.0$, for all path frequencies ($p \leq 0.025$; Fig. 5B; Table 2), but corrected step width deviations, $M(w)$, similarly on the STR paths ($p = 0.957$; Fig. 5D; Table 2), but less so, $M(w) \rightarrow 0.0$, on the LOF and HIF paths ($p \leq 0.012$; Fig. 5D; Table 2).

As path oscillation frequency increased from STR to LOF paths, participants corrected z_B deviations less ($\uparrow M(z_B)$) for both path widths ($p < 0.001$; Fig. 5B; Table 2) and corrected w deviations more ($\downarrow M(w)$) for the wide path ($p < 0.001$), but only somewhat more for the narrow path ($p = 0.070$) (Fig. 5D; Table 2). As path oscillation frequency increased further from LOF to HIF paths, participants corrected z_B deviations much more ($\downarrow M(z_B)$) for both path widths ($p < 0.001$; Fig. 5B; Table 2) and also corrected w deviations more ($\downarrow M(w)$) for the narrow path ($p < 0.001$), but not for the wide path ($p = 0.539$) (Fig. 5D; Table 2).

[Insert Figure 5 About Here]

GEM-Relevant Variance

On the STR and LOF paths, participants much more strongly corrected step width deviations (Fig. 5D) than position deviations (Fig. 5B). As expected (Dingwell and Cusumano, 2019), this yielded variance distributions in the [z_L, z_R] plane strongly aligned with the w^* GEM: i.e., $\sigma(z_B)/\sigma(w) \gg 1$ (Fig. 6).

On the narrow paths for these STR and LOF frequency conditions, however, as participants decreased their w-regulation to increase z_B-regulation (Fig. 5), their variance distributions became significantly more isotropic ($p < 0.001$; $\sigma(z_B)/\sigma(w) \rightarrow 1$; Fig. 6; Table 2).

On the HIF paths, as participants strongly corrected deviations in both lateral position (Fig. 5B) and step width (Fig. 5D), their variance distributions became significantly more isotropic ($\sigma(z_B)/\sigma(w) \approx 1$) than for either STR or LOF (p

< 0.001; Fig. 6; Table 2) and for both path widths (p = 0.102; Fig. 6; Table 2).

[Insert Figure 6 About Here]

Correlations With Baseline Measures

Having faster FSST times predicted, for the Narrow HIF path condition, stronger lateral position error correction (↓ $M(z_B)$; $R^2 = 27.4\%$, p = 0.01), coupled with somewhat weaker step width error correction (↑ $M(w)$; $R^2 = 16.2\%$, p = 0.06), which resulted in more strongly position-biased variance distributions ($\sigma(z_B)/\sigma(w) < 1$; $R^2 = 49.0\%$, p < 0.001) (Fig. 7). Having slower 4CRT reaction times (not shown) predicted qualitatively similar (though somewhat less statistically significant) performance in this Narrow HIF path walking task.

[Insert Figure 7 About Here]

DISCUSSION

Being able to walk around turns or through narrow or crowded spaces are important for our daily mobility (Musselman and Yang, 2007). Walking is goal-directed (Arechavaleta et al., 2008) and people employ multi-objective lateral stepping regulation (Dingwell and Cusumano, 2019) to adapt to specific environmental conditions and tasks. People readily modulate their lateral foot placements given explicit feedback (Render et al., 2021), while walking on narrowing paths (Kazanski et al., 2023), and performing discrete lateral maneuvers (Acasio et al., 2017; Desmet et al., 2022). Here, we asked people to walk on continuously-winding pathways. We aimed to determine how people balanced the competing task goals, maintain step width or lateral position, in environments designed to demand both simultaneously. We utilized our GEM framework for lateral stepping to quantify how people modify stepping regulation and the resulting variance structures on both narrow and winding walking paths.

When walking on the Narrow paths, people took narrower steps (Fig. 3B) with less lateral position variability (Fig. 4A). People did not decrease their step width variability on the narrower straight path (Fig. 4B; STR), similar to (Arvin et al., 2016; Schrager et al., 2008), but they did on the narrower winding paths (Fig. 4B). Results confirmed our first prediction that, on the narrower paths, people would trade off decreased w-regulation for increased z_B-regulation, as we found previously for continuously-narrowing paths (Kazanski et al., 2023). Specifically, people corrected deviations in their lateral position *more* (Fig. 5B), while correcting deviations in step width *less* (Fig. 5D). That people made this trade-off was also reflected in the variance structure of their stepping data plotted in the [z_L, z_R] plane (Fig. 6), where for the STR and LOF conditions particularly, the $\sigma(z_B)/\sigma(w)$ variance ratios decreased closer to 1 on the narrower paths.

Path sinuosity also altered lateral stepping. While navigating more sinuous paths, people took both narrower (Fig. 3B) and more variable (Fig. 4A-B) steps. Interestingly, on the LOF winding paths, people traded-off correcting deviations in their step width *more* (Fig. 5C-D) at the expense of correcting deviations in their lateral position *less* (Fig. 5A-B). This was also reflected in the $\sigma(z_B)/\sigma(w)$ ratios that were higher in LOF than STR (Fig. 6A-B). Thus, on these moderately-challenging LOF winding paths, people increased their prioritization of maintaining step width, likely to maintain lateral balance.

Consistent with our second prediction, on more sinuous winding paths (HIF) people more strongly corrected errors in both lateral position (Fig. 5A-B) *and* step width (Fig. 5C-D), very similar to what people do when subjected to external (mechanical or visual) lateral perturbations (Kazanski et al., 2020). Critically, however, in (Kazanski et al., 2020), those perturbations were both unpredictable and externally imposed. Conversely, here, people could see their upcoming paths well in advance (Matthis et al., 2017), so their stepping movements were both readily

predictable and internally planned (Drew and Marigold, 2015). Our findings thus demonstrate that whether reactive or anticipatory, people adopt similar stepping regulation strategies both when responding to external perturbations and when executing pre-planned tasks.

That people adopted these stepping regulation strategies was also reflected in the variance structure of their stepping data plotted in the [z_L, z_R] plane (Fig. 6), where on the HIF paths, their $\sigma(z_B)/\sigma(w)$ variance ratios were much closer to 1 for both path widths. Similarly close-to-isotropic [z_L, z_R] plane variance distributions were observed when people performed discrete lateral maneuvers (Desmet et al., 2024) or walked on narrowing paths (Kazanski et al., 2023). Thus, on these more-challenging HIF winding paths, people prioritized maintaining both lateral balance *and* lateral position to similar degrees, likely to maximize their maneuverability (Acasio et al., 2017; Desmet et al., 2022).

Furthermore, the four-square step test (FSST) is a specific functional clinical test of lateral maneuverability (Dite and Temple, 2002). Here, those participants who executed faster FSST times also corrected position (z_B) errors more and step width (w) errors less, which consequently yielded [z_L, z_R] variance distributions biased more towards z_B-regulation (Fig. 7). Hence, those who exhibited stepping patterns that more effectively traded-off stability for maneuverability (Desmet et al., 2022; Desmet et al., 2024) also exhibited faster FSST times. The correlations shown in Fig. 7 thus offer strong evidence of the *concurrent validity* (Portney and Watkins, 2015) of these lateral stepping regulation measures. Greater ability to adapt one's lateral stepping regulation to enhance maneuverability appears an important contributor to being able to perform functional balance tests like the FSST faster. The analyses presented here thus reveal important stepping regulation mechanisms people use to achieve better performance in such functional tasks.

For individuals with gait impairments, many prior studies and clinical training programs have subjected individuals to perturbations (Mansfield et al., 2015). However, based on findings from (Robinovitch et al., 2013), circumstances of falls do not always involve external perturbations. Often, people fall from negotiating a maneuver improperly (Ambrose et al., 2013). Our findings here support that walking paradigms that vary path width and sinuosity may offer more ecologically valid and effective gait interventions to target specific adaptive strategies that improve overall balance and mobility.

REFERENCES

Acasio, J., Wu, M.M., Fey, N.P., Gordon, K.E., 2017. Stability-maneuverability trade-offs during lateral steps. Gait Posture 52, 171-177.

Ambrose, A.F., Paul, G., Hausdorff, J.M., 2013. Risk factors for falls among older adults: A review of the literature. Maturitas 75, 51-61.

Arechavaleta, G., Laumond, J.P., Hicheur, H., Berthoz, A., 2008. An Optimality Principle Governing Human Walking. IEEE Trans Robot. 24, 5-14.

Arvin, M., Mazaheri, M., Hoozemans, M.J.M., Pijnappels, M., Burger, B.J., Verschueren, S.M.P., van Dieën, J.H., 2016. Effects of narrow base gait on mediolateral balance control in young and older adults. J. Biomech. 49, 1264-1267.

Bauby, C.E., Kuo, A.D., 2000. Active Control of Lateral Balance in Human Walking. J. Biomech. 33, 1433-1440.

Bohnsack-McLagan, N.K., Cusumano, J.P., Dingwell, J.B., 2016. Adaptability of Stride-To-Stride Control of Stepping Movements in Human Walking. J. Biomech. 49, 229-237.

Bruijn, S.M., van Dieën, J.H., 2018. Control of human gait stability through foot placement. J. R. Soc. Interface 15, 1-11.

Cusumano, J.P., Cesari, P., 2006. Body-Goal Variability Mapping in an Aiming Task. Biol. Cybern. 94, 367-379.

Cusumano, J.P., Dingwell, J.B., 2013. Movement Variability Near Goal Equivalent Manifolds: Fluctuations, Control, and Model-Based Analysis. Hum. Mov. Sci. 32, 899-923.

Desmet, D.M., Cusumano, J.P., Dingwell, J.B., 2022. Adaptive Multi-Objective Control Explains How Humans Make Lateral Maneuvers While Walking. PLoS Comput. Biol. 18, e1010035.

Desmet, D.M., Kazanski, M.E., Cusumano, J.P., Dingwell, J.B., 2024. How Healthy Older Adults Enact Lateral Maneuvers While Walking. Gait Posture 108, 117-123.

Dingwell, J.B., Cusumano, J.P., 2015. Identifying Stride-To-Stride Control Strategies in Human Treadmill Walking. PLoS ONE 10, e0124879.

Dingwell, J.B., Cusumano, J.P., 2019. Humans Use Multi-Objective Control to Regulate Lateral Foot Placement When Walking. PLoS Comput. Biol. 15, e1006850.

Dingwell, J.B., Cusumano, J.P., Rylander, J.H., Wilken, J.M., 2021. How Persons With Transtibial Amputation Regulate Lateral Stepping While Walking in Laterally Destabilizing Environments. Gait Posture 83, 88-95.

Dingwell, J.B., John, J., Cusumano, J.P., 2010. Do Humans Optimally Exploit Redundancy to Control Step Variability in Walking? PLoS Comput. Biol. 6, e1000856.

Dingwell, J.B., Render, A.C., Desmet, D.M., Cusumano, J.P., 2023. Generalizing Stepping Concepts to Non-Straight Walking. J. Biomech. 161, 111840.

Dite, W., Temple, V.A., 2002. A clinical test of stepping and change of direction to identify multiple falling older adults. Arch. Phys. Med. Rehabil. 83, 1566-1571.

Drew, T., Marigold, D.S., 2015. Taking the next step: cortical contributions to the control of locomotion. Current Opinion in Neurobiology 33, 25-33.

Glaister, B.C., Bernatz, G.C., Klute, G.K., Orendurff, M.S., 2007. Video task analysis of turning during activities of daily living. Gait Posture 25, 289-294.

Ho, T.K., Kreter, N., Jensen, C.B., Fino, P.C., 2023. The choice of reference frame alters interpretations of turning gait and stability. J. Biomech. 151, 111544.

Kazanski, M.E., Cusumano, J.P., Dingwell, J.B., 2020. How Healthy Older Adults Regulate Lateral Stepping While Walking in Laterally Destabilizing Environments. J. Biomech. 104, 109714.

Kazanski, M.E., Cusumano, J.P., Dingwell, J.B., 2023. How Older Adults Regulate Lateral Stepping on Narrowing Walking Paths. J. Biomech. 160, 111836.

Kuo, A.D., 1999. Stabilization of Lateral Motion in Passive Dynamic Walking. Int. J. Robotics Res. 18, 917-930.

MacKinnon, C.D., Winter, D.A., 1993. Control of Whole Body Balance In The Frontal Plane During Human Walking. J. Biomech. 26, 633-644.

Mansfield, A., Wong, J.S., Bryce, J., Knorr, S., Patterson, K.K., 2015. Does Perturbation-Based Balance Training Prevent Falls? Systematic Review and Meta-Analysis of Preliminary Randomized Controlled Trials. Phys. Ther. 95, 700-709.

Matthis, J.S., Barton, S.L., Fajen, B.R., 2017. The critical phase for visual control of human walking over complex terrain. Proc. Natl. Acad. Sci. USA 114, E6720-E6729.

Matthis, J.S., Yates, J.L., Hayhoe, M.M., 2018. Gaze and the Control of Foot Placement When Walking in Natural Terrain. Curr. Biol. 28, 1224-1233.e1225.

McAndrew, P.M., Wilken, J.M., Dingwell, J.B., 2011. Dynamic Stability of Human Walking in Visually and Mechanically Destabilizing Environments. J. Biomech. 44, 644-649.

Moussaïd, M., Helbing, D., Theraulaz, G., 2011. How simple rules determine pedestrian behavior and crowd disasters. Proc. Natl. Acad. Sci. USA 108, 6884-6888.

Mueller, S.T., Piper, B.J., 2014. The Psychology Experiment Building Language (PEBL) and PEBL Test Battery. J. Neurosci. Meth. 222, 250-259.

Musselman, K.E., Yang, J.F., 2007. Walking tasks encountered by urban-dwelling adults and persons with incomplete spinal cord injuries. J. Rehabil. Med. 39, 567-574.

Olivier, A.-H., Marin, A., Crétual, A., Berthoz, A., Pettré, J., 2013. Collision avoidance between two walkers: Role-dependent strategies. Gait Posture 38, 751-756.

Orendurff, M.S., Schoen, J.A., Bernatz, G.C., Segal, A.D., Klute, G.K., 2008. How Humans Walk: Bout Duration, Steps per Bout, and Rest Duration. J. Rehabil. Res. Develop. 45, 1077-1090.

Patil, N.S., Dingwell, J.B., Cusumano, J.P., 2022. Viability, Task Switching, and Fall Avoidance of the Simplest Dynamic Walker. Scientific Reports 12, 8993.

Pham, Q.-C., Berthoz, A., Hicheur, H., 2011. Invariance of Locomotor Trajectories Across Visual and Gait Direction Conditions. Exp. Brain Res. 210, 207-215.

Portney, L.G., Watkins, M.P., 2015. Foundations of Clinical Research: Applications to Practice, 3rd. ed. F. A. Davis Co., Philadelphia, PA.

Render, A.C., Kazanski, M.E., Cusumano, J.P., Dingwell, J.B., 2021. Walking humans trade off different task goals to regulate lateral stepping. J. Biomech. 119, 110314.

Richards, J., Levine, D., Whittle, M.W., 2023. Whittle's Gait Analysis, 6th Ed. Elsevier.

Robinovitch, S.N., Feldman, F., Yang, Y., Schonnop, R., Leung, P.M., Sarraf, T., Sims-Gould, J., Loughin, M., 2013. Video capture of the circumstances of falls in elderly people residing in long-term care: an observational study. Lancet 381, 47-54.

Schrager, M.A., Kelly, V.E., Price, R., Ferrucci, L., Shumway-Cook, A., 2008. The effects of age on medio-lateral stability during normal and narrow base walking. Gait Posture 28, 466-471.

Townsend, M.A., 1985. Biped Gait Stabilization Via Foot Placement. J. Biomech. 18, 21-38.

Twardzik, E., Duchowny, K., Gallagher, A., Alexander, N., Strasburg, D., Colabianchi, N., Clarke, P., 2019. What features of the built environment matter most for mobility? Using wearable sensors to capture real-time outdoor environment demand on gait performance. Gait Posture 68, 437-442.

Zeni, J.A., Richards, J.G., Higginson, J.S., 2008. Two simple methods for determining gait events during treadmill and overground walking using kinematic data. Gait Posture 27, 710-714.

TABLES & FIGURES:

Table 1. Participant physical characteristics and assessment scores. Dynamic balance ability and coordination was assessed using the Four-Square Step Test (FSST). Attention and processing speed was assessed using the Four-Choice Reaction Time (4CRT) test. All values except Sex are given as Mean ± Standard Deviation.

Characteristic:	**Value:**
Sex [F/M]	12 / 12
Age [yrs]	25.8 ± 3.5
Body Height [m]	1.74 ± 0.11
Body Mass [kg]	70.15 ± 14.75
Leg Length [m]	0.93 ± 0.05
Assessment:	
FSST [s]	6.10 ± 0.043
4CRT [ms]	384.6 ± 77.9

Table 2. Statistical results for differences between path Frequencies (STR, LOF, and HIF) and path Widths (Wide, Narrow) for data shown in Figs. 3-6. ANOVA results (F-statistics and p-values) are provided for main effects of Frequency and Width, and for Frequency × Width interactions. Tukey's post-hoc comparisons are presented where relevant. Significant differences are indicated in bold.

* In cases where Frequency × Width interactions were significant, we considered main effects results to be unreliable and potentially misleading. We drew conclusions instead from the Tukey's pairwise comparisons, as these account for the effects of the interactions.

Data In	Variable	Frequency	Width	Frequency × Width	Tukey's (Frequency Effects)	Tukey's (Width Effects)
Fig. 3A:	$\mu(z_B)$	$F_{(2,259)} = 2.44$ $p = 0.089$	$F_{(1,259)} = 0.37$ $p = 0.546$	$F_{(2,259)} = 0.38$ $p = 0.686$	N/A	N/A
Fig. 3B:	$\mu(w)$	$F_{(2,259)} = 151.01$ $p^* < 0.001$	$F_{(1,259)} = 377.43$ $p^* < 0.001$	$F_{(2,259)} = 6.10$ **$p = 0.003$**	**STRW-LOFW: $p = 0.001$** **STRW-HIFW: $p < 0.001$** **LOFW-HIFW: $p < 0.001$** **STRN-LOFN: $p = 0.001$** **STRN-HIFN: $p < 0.001$** **LOFN-HIFN: $p < 0.001$**	**STRW-STRN: $p < 0.001$** **LOFW-LOFN: $p < 0.001$** **HIFW-HIFN: $p < 0.001$**
Fig. 4A:	$\sigma(z_B)$	$F_{(2,259)} = 1116.41$ $p^* < 0.001$	$F_{(1,259)} = 807.47$ $p^* < 0.001$	$F_{(2,259)} = 64.99$ **$p = < 0.001$**	**STRW-LOFW: $p < 0.001$** **STRW-HIFW: $p < 0.001$** **LOFW-HIFW: $p < 0.001$** **STRN-LOFN: $p < 0.001$** **STRN-HIFN: $p < 0.001$** **LOFN-HIFN: $p < 0.001$**	**STRW-STRN: $p < 0.001$** **LOFW-LOFN: $p < 0.001$** **HIFW-HIFN: $p < 0.001$**
Fig. 4B:	$\sigma(w)$	$F_{(2,259)} = 2200.36$ $p^* < 0.001$	$F_{(1,259)} = 206.74$ $p^* < 0.001$	$F_{(2,259)} = 85.57$ **$p = < 0.001$**	**STRW-LOFW: $p = 0.001$** **STRW-HIFW: $p < 0.001$** **LOFW-HIFW: $p < 0.001$** **STRN-LOFN: $p = 0.011$** **STRN-HIFN: $p < 0.001$** **LOFN-HIFN: $p < 0.001$**	STRW-STRN: $p = 0.115$ **LOFW-LOFN: $p = 0.011$** **HIFW-HIFN: $p < 0.001$**
Fig. 5B:	$M(z_B)$	$F_{(2,259)} = 1676.69$ $p^* < 0.001$	$F_{(1,259)} = 193.95$ $p^* < 0.001$	$F_{(2,259)} = 18.28$ **$p = < 0.001$**	**STRW-LOFW: $p < 0.001$** **STRW-HIFW: $p < 0.001$** **LOFW-HIFW: $p < 0.001$** **STRN-LOFN: $p < 0.001$** **STRN-HIFN: $p < 0.001$** **LOFN-HIFN: $p < 0.001$**	**STRW-STRN: $p < 0.001$** **LOFW-LOFN: $p < 0.001$** **HIFW-HIFN: $p = 0.025$**
Fig. 5D:	$M(w)$	$F_{(2,259)} = 91.67$ $p^* < 0.001$	$F_{(1,259)} = 67.43$ $p^* < 0.001$	$F_{(2,259)} = 22.58$ **$p = < 0.001$**	**STRW-LOFW: $p < 0.001$** **STRW-HIFW: $p < 0.001$** LOFW-HIFW: $p = 0.539$ STRN-LOFN: $p = 0.070$ **STRN-HIFN: $p < 0.001$** **LOFN-HIFN: $p < 0.001$**	STRW-STRN: $p = 0.957$ **LOFW-LOFN: $p < 0.001$** **HIFW-HIFN: $p = 0.012$**
Fig. 6B:	$\sigma(z_B)/\sigma(w)$	$F_{(2,259)} = 566.36$ $p^* < 0.001$	$F_{(1,259)} = 238.25$ $p^* < 0.001$	$F_{(2,259)} = 42.36$ **$p = < 0.001$**	**STRW-LOFW: $p < 0.001$** **STRW-HIFW: $p < 0.001$** **LOFW-HIFW: $p < 0.001$** **STRN-LOFN: $p < 0.001$** **STRN-HIFN: $p < 0.001$** **LOFN-HIFN: $p < 0.001$**	**STRW-STRN: $p < 0.001$** **LOFW-LOFN: $p < 0.001$** HIFW-HIFN: $p = 0.102$

Figure 1. A) Photo of a participant walking in a Motek M-Gait virtual reality system. **(B)** Schematic indicating a path (here, straight/STR) projected onto the treadmill surface. Global coordinates are $+x$ forward, $+y$ vertical up, and $+z$ to the right. **C)** Participants traversed paths of each of three oscillation frequency combinations, Eq. (1): straight (STR; grey panel), low (LOF; red panel), and high (HIF; purple panel). Each path frequency was tested at two different widths, "Wide" (W; path width = 0.6 m; beige) and "Narrow" (N; path width = 0.3 m; yellow), for a total of six conditions tested for each participant.

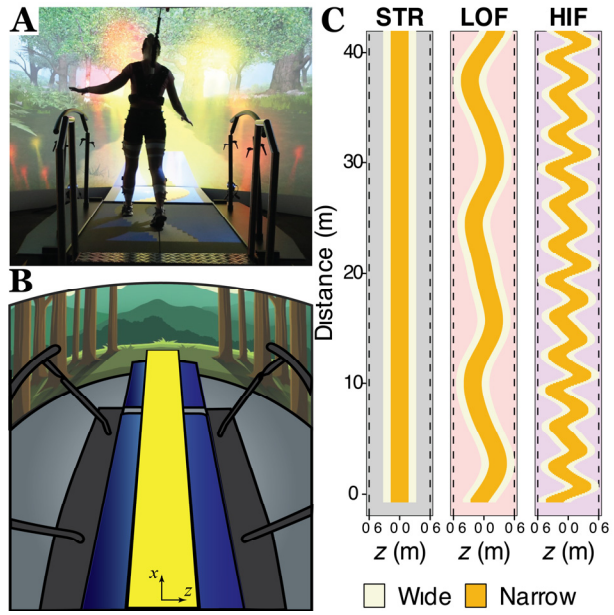

Figure 2. A) At each step, we rotate the lab-defined global coordinate system, $[x,z]$ to define a path-aligned local coordinate system, $[x',z']$ in which the x' axis is tangent to the path closest to the midpoint between the two feet (Dingwell et al. 2023). The locally lateral positions of the left and right feet $\{z'_L, z'_R\}$ are used to derive the lateral body position as the midpoint, $z_B = ½(z'_L + z'_R)$, and step width as the difference, $w = z'_R - z'_L$. **B**) Example time series data of path-aligned z_B (green) and w (blue) for a representative trial from a typical participant. For the z_B plot (left), the grey vertical dashed line indicates the center of the path (i.e., $z_B = 0$). **C**) Example direct control plot used to quantify how people correct errors in $q \in \{z_B, w\}$ from step-to-step: deviations from the mean on a given step, on, $\tilde{q}_{(n)} = q_{(n)} - q^*$, are plotted (yellow markers) against the corrections made on the subsequent step, $\Delta q_{(n+1)} = q_{(n+1)} - q_n$. The solid yellow diagonal line indicates the error correction slope, $M(q)$, computed via linear least-squares. The black dashed line indicates "perfect" error correction ($M(q) = -1$). **D**) Lateral foot placements (yellow markers) plotted in $[z_L, z_R]$ plane for a typical trial. Stepping regulation variables $[z_B, w]$ map onto $[z_L, z_R]$ as mutually orthogonal GEMs representing constant lateral body position (z_B^* = constant; green) and constant step width (w^* = constant; blue): position variability, $\sigma(z_B)$ quantifies deviations along w^*, whereas step width variability, $\sigma(w)$, quantifies deviations along z_B^*.

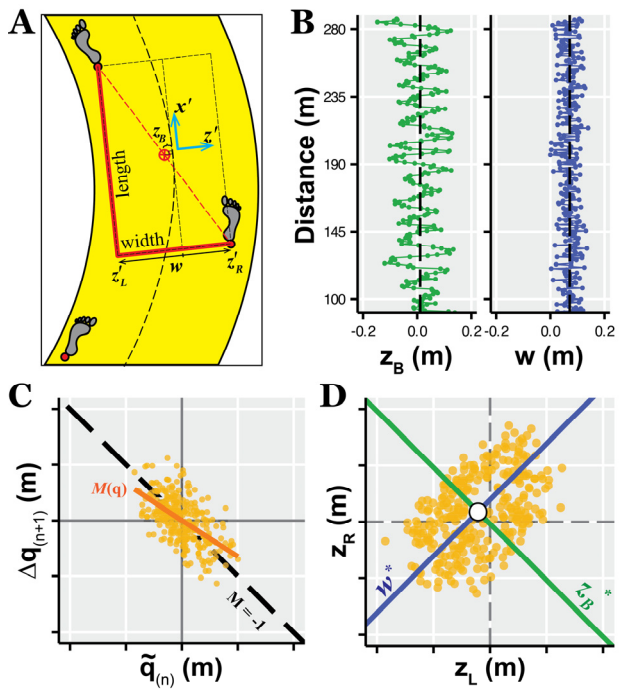

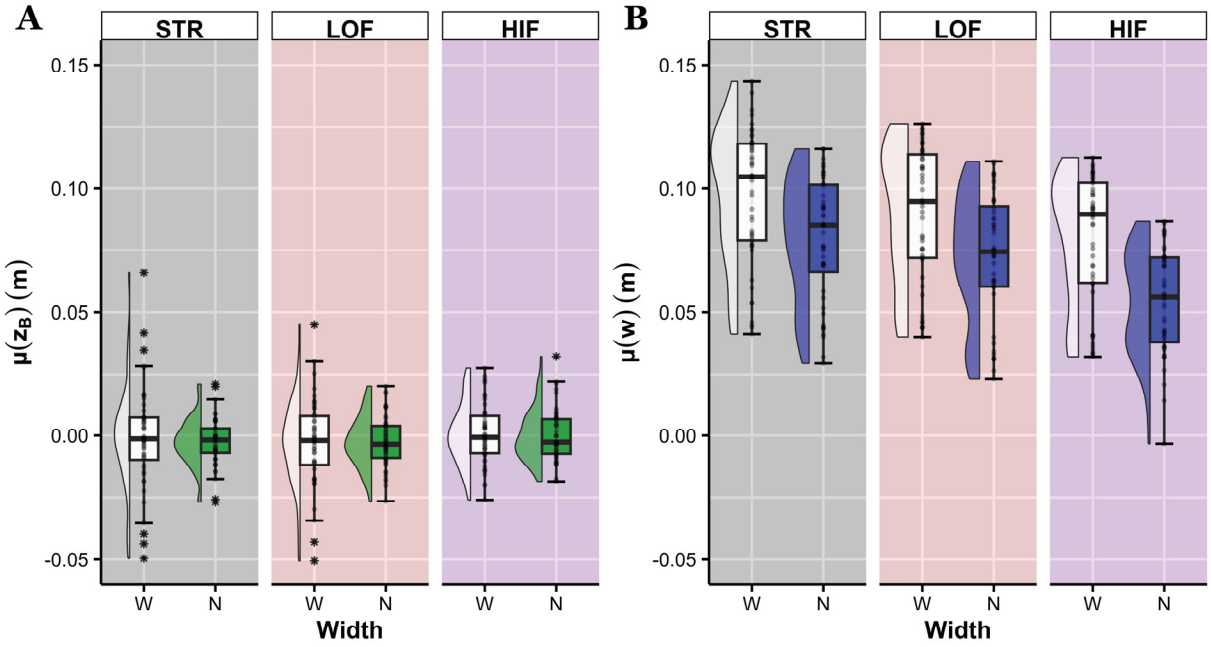

Figure 3. Mean values for (**A**) lateral body position, $\mu(z_B)$, and (**B**) step width, $\mu(w)$, on wide (W) and narrow (N) paths for each path oscillation frequency: STR (grey), LOF (red), and HIF (purple). Box plots show the medians, 1st and 3rd quartiles, and whiskers extending to 1.5 × interquartile range. Values beyond this range are shown as individual asterisks. The overlaid markers are individual data points for each participant from two separate trials**.** Half-violin plots in each subplot show estimated probability density functions for visual reference. Results of statistical comparisons are in Table 2.

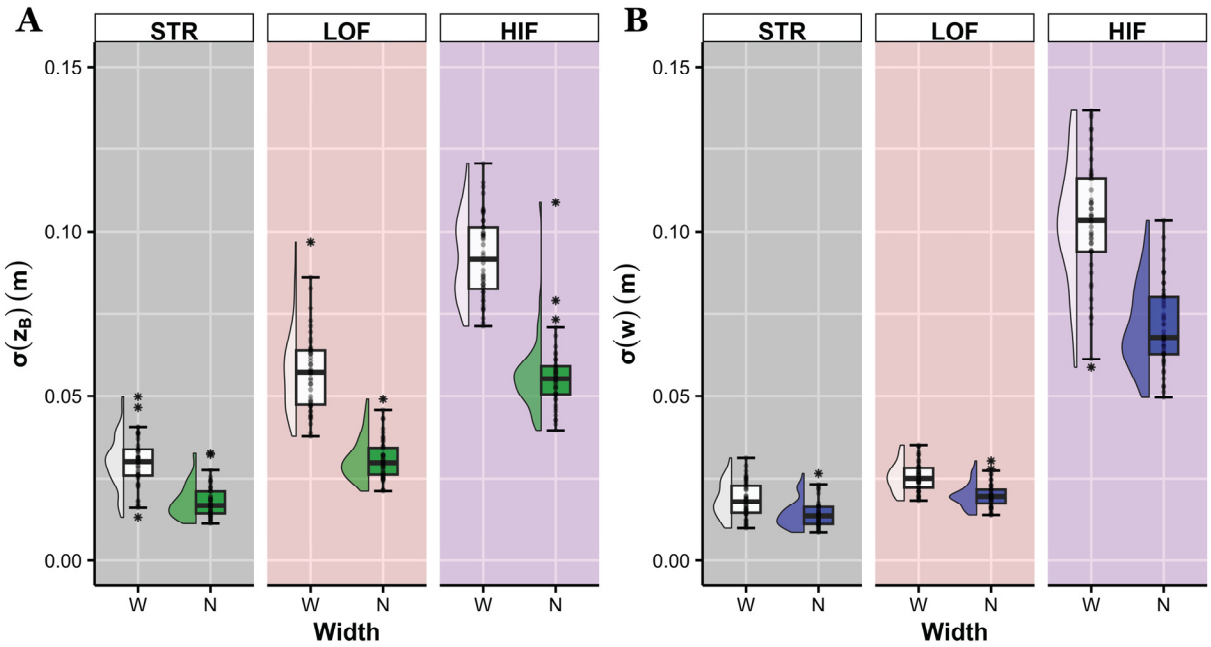

Figure 4. Within-trial standard deviations for (**A**) lateral body position, $\sigma(z_B)$, and (**B**) step width, $\sigma(w)$, on wide (W) and narrow (N) paths for each path oscillation frequency. Data are plotted in the same manner as in Fig. 3. Results of statistical comparisons are in Table 2.

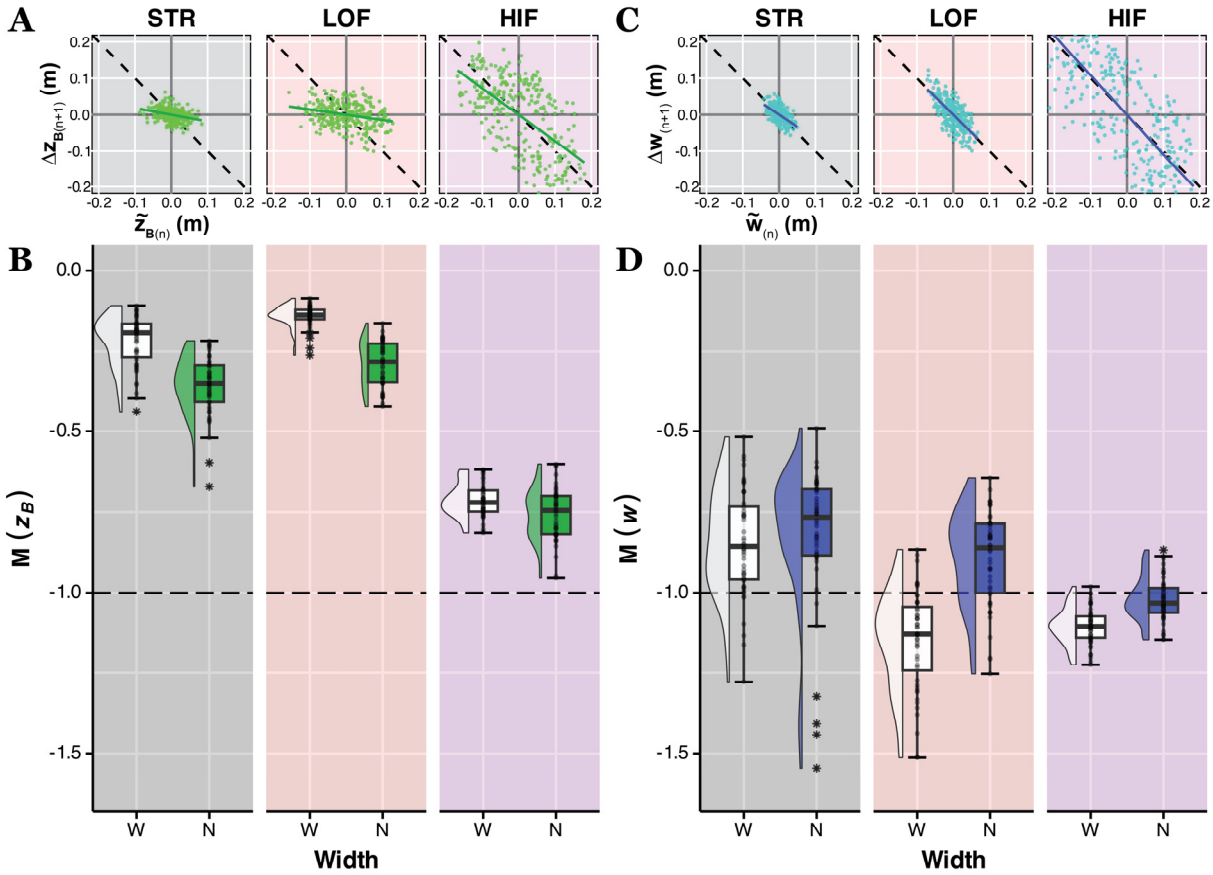

Figure 5. Representative direct control plots of $\tilde{q}_{(n)}$ vs. $\Delta q_{(n+1)}$ (see Fig. 2C) from a typical participant walking on the three different Wide paths for (**A**) lateral body position ($q \equiv z_B$) and (**C**) step width ($q \equiv w$). Group data for linear error correction slopes for (**B**) lateral body positions, $M(z_B)$, and (**D**) step widths, $M(w)$, on the wide (W) and narrow (N) paths for each oscillation frequency: STR (grey), LOF (red), and HIF (purple) for all trials and participants, plotted in the same manner as in Figs. 3-4. Horizontal dashed lines at slope $M = -1$ indicate perfect error correction: i.e., values above this line reflect *under*-correction, whereas values below this line reflect *over*-correction. Results of statistical comparisons are in Table 2.

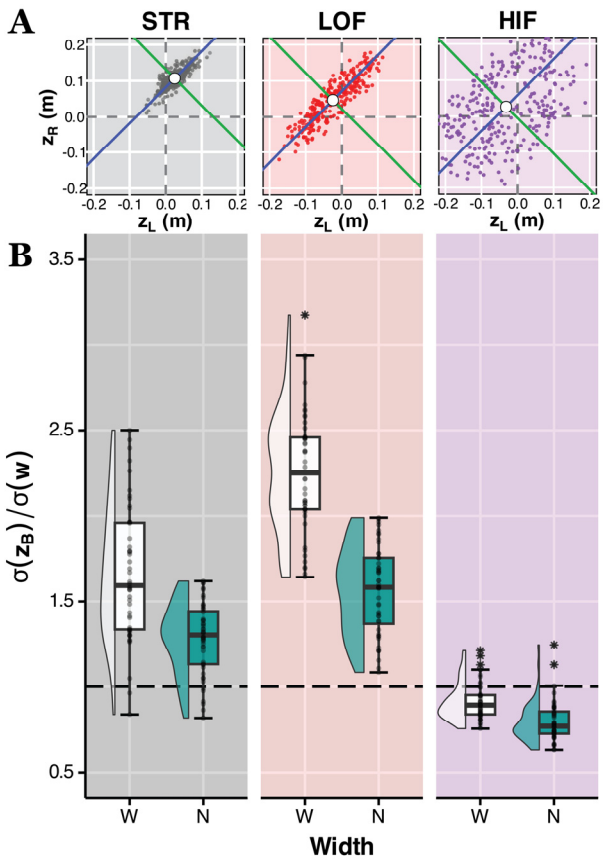

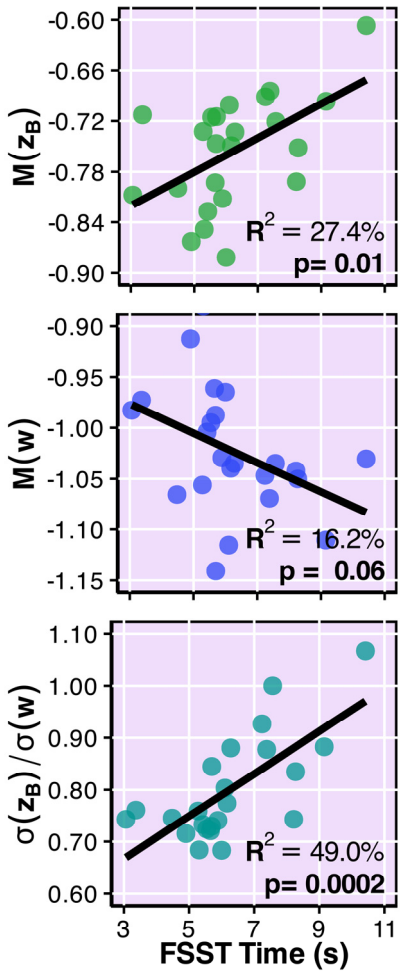

Figure 6. A) Example lateral foot placements plotted in [z_L, z_R] plane (see Fig. 2D) from a typical participant walking on the Wide paths. **B**) Group data for the ratio of lateral body position to step width variances, $\sigma(z_B)/\sigma(w)$, for all trials and participants, plotted in the same manner as in Figs. 3-4. Horizontal dashed lines at $\sigma(z_B)/\sigma(w) = +1$ indicate isotropic variance distributions. Results of statistical comparisons are in Table 2.

Figure 7. Linear correlations between participants' baseline average Four-Square Step Test (FSST; Table 1) times and their average $M(z_B)$ slopes, $M(w)$ slopes, and $\sigma(z_B)/\sigma(w)$ ratios when walking in the Narrow HIF path condition. In each plot, single markers indicate the average values for each participant. Black solid straight lines indicate linear best fit lines. Correlation strengths (R^2) and statistical significance (p-values) for each relationship are indicated on each sub-plot.